Int. J. Heat Mass Transfer. Vol. 8, pp. 1281–1301. Pergamon Press 1965. Printed in Great Britain

HEAT TRANSFER AND FRICTION FOR LAMINAR FLOW OF GAS IN A CIRCULAR TUBE AT HIGH HEATING RATE

SOLUTIONS FOR HYDRODYNAMICALLY DEVELOPED FLOW BY A FINITE-DIFFERENCE METHOD

P. M. WORSØE-SCHMIDT† and G. LEPPERT

Department of Mechanical Engineering, Stanford University, California

(*Received* 1 *February* 1965 *and in revised form* 23 *April* 1965)

Abstract—An implicit finite difference scheme is developed for solving the problem of laminar flow of gases in heated (or cooled) circular tubes with an unheated entrance section, under conditions where large variations of gas properties occur. The solution is based on the boundary-layer equations, the validity of which for the present problem has been verified from the numerical solutions.

Numerical examples are worked out for air including (i) pure forced convection with different rates of uniform heating; (ii) pure forced convection with uniform wall temperature with heating as well as cooling of the gas; and (iii) superimposed forced and natural convection with uniform heat flux. For pure forced convection approximate expressions for the local Nusselt number and the friction factor are given.

NOMENCLATURE

Lower case letters

a, exponent in power law for specific heat;
b, exponent in power law for viscosity;
c, exponent in power law for thermal conductivity;
c_p, specific heat at constant pressure;
c_p^+, non-dimensional specific heat, $c_p/c_{p,0}$;
c_v, specific heat at constant volume;
f, friction factor, $\tau_w/[\frac{1}{2}(\rho u)_m u_m]$;
g, acceleration of gravity;
k, thermal conductivity;
k^+, non-dimensional thermal conductivity, k/k_0;
m, designation of arbitrary mesh point in the axial direction;
n, designation of arbitrary mesh point in the radial direction;
p, absolute pressure;
p^+, non-dimensional pressure, p/p_0;
q_w'', heat flux at tube wall;
q^+, non-dimensional heat flux, $r_0 q_w''/(k_0 T_0)$;
r, radial coordinate;
r^+, non-dimensional radial coordinate, r/r_0;
r_0, tube radius;
u, axial velocity;
u^+, non-dimensional axial velocity, u/u_0;
u_0, mean velocity at $x = 0$;
v, radial velocity;
v^+, non-dimensional radial velocity, $(v/u_0)N_{Re,0}\,N_{Pr,0}$;
x, axial coordinate;
x^+, non-dimensional axial coordinate, $(x/r_0)/(N_{Re,0}\,N_{Pr,0})$.

Capital letters

D, tube diameter;
H, enthalpy;
H^+, non-dimensional enthalpy, $(H - H_0)/(c_{p,0}\,T_0)$;
M_0, Mach number, $u_0/(\gamma_0 R T_0)^{1/2}$;
N, designation of mesh points on the wall;
N_E, parameter in energy equation, $(\gamma_0 - 1)M_0^2$;
N_G, parameter in momentum equation, $N_{Gr^*,0}\,N_{Pr,0}/N_{Re,0}$;

† On leave from The Technical University of Denmark. Present address: Department of Mechanical Engineering, The Technical University of Denmark, Copenhagen.

N_{Gr}, Grashof number, $8g\rho^2(T_w - T_m)r_0^3/(T_m\mu^2)$;
N_{Gr*}, modified Grashof number, $8g\rho^2 r_0^3/\mu^2$:
N_{Nu}, Nusselt number, $2q_w'' r_0/[k(T_w - T_m)]$;
N_{Pe}, Péclet number, $N_{Re}\,N_{Pr}$;
$N_{Pe,x}$, Péclet number, based on axial distance, $N_{Re,x}\,N_{Pr}$;
N_{Pr}, Prandtl number, $\mu c_p/k$;
N_{Re}, Reynolds number, $2(\rho u)_m r_0/\mu$;
$N_{Re,x}$, Reynolds number, based on axial distance, $2\rho_0 u_0 x/\mu_0$;
P, pressure defect, $(p - p_0)/(\rho_0 u_0^2) = (1 - p^+)/(\gamma_0 M_0^2)$;
R, gas constant;
T, absolute temperature.

Greek symbols

γ, ratio of specific heats, c_p/c_v;
δ, central difference operator;
$\Delta x, \Delta r$ step-widths in axial and radial direction respectively;
$\Delta x^+, \Delta r^+$, non-dimensional step-widths;
θ, non-dimensional temperature, T/T_0;
μ, viscosity;
μ^+, non-dimensional viscosity, μ/μ_0;
ρ, density;
ρ^+, non-dimensional density, ρ/ρ_0;
σ, weighting factor in difference quotients;
τ_w, wall shear stress, $-\left(\mu \dfrac{\partial u}{\partial r}\right)_{r=r_0}$;
τ_w^+, non-dimensional wall shear stress, $-\left(\mu^+ \dfrac{\partial u^+}{\partial r^+}\right)_{r^+=1}$;
ϕ, arbitrary dependent variable.

Subscripts

m, mean value (with respect to cross section); evaluated at the mixed mean temperature; in difference equations, referring to $x = m\Delta x$;
n, referring to $r = n\Delta r$;
N, referring to mesh points on the wall;
0, for gas properties, reference value at $x = 0$; for non-dimensional parameters, evaluated at $x = 0$;
x, Reynolds and Péclet numbers based on axial distance from $x = 0$;
w, evaluated at the tube wall.

INTRODUCTION

IN RECENT YEARS high temperature heat transfer to gases has attracted considerable interest, notably in connection with cooling of nuclear reactors. Due to the variation of the physical properties of the gas, over the cross-section of the duct as well as axially, that occurs at high heating rates, the classical solutions which are based on the assumption of constant fluid properties may lead to serious errors in the predicted performance.

For gases both the density and the transport coefficients are, at least approximately, proportional to the absolute temperature of the gas raised to some power. The ratio of the absolute temperature of the wall and of the gas (e.g. the mixed mean, or bulk, temperature), respectively, is therefore a good indication of whether the property variation is significant or not. As long as this ratio is less than approximately 1·2 constant-properties solutions will give reasonably accurate results for the heat transfer.

The first attempt to solve the problem of laminar flow of gases with appreciable (radial) variation of both thermodynamic and transport properties was made by Deissler [1] who based his solution, for uniform heat flux at the wall, on the concept of fully developed velocity and temperature profiles. Later a similar analysis has been carried out by Sze [2]. Davenport and Leppert [3] assumed that sufficiently far from the entrance quasi-developed velocity and temperature profiles existed and included in their analysis the effect of a radial velocity component. Koppel and Smith [4] obtained an approximate finite-difference solution for laminar flow of carbon dioxide near its critical point.

Experimental heat-transfer data for both heating and cooling of air with wall-to-bulk temperature ratios between 0·5 and 2 have been presented by Kays and Nicoll [5]. Davenport and Leppert [3] measured both heat transfer and pressure drop for flow of nitrogen and helium with wall-to-bulk temperature ratios up to 2·2. Heat-transfer and friction data have also been reported by Dalle Donne and Bowditch [6, 7] for flow of air and helium with maximum wall-to-bulk temperature ratios of a little over two.

The trend in the experimental results is consistently that up to the highest temperature ratio

attained so far, Nusselt numbers evaluated at the mixed mean temperature deviate less from the corresponding values for constant properties than predicted by the analyses of references 1 and 2. The deviations are, in fact, almost completely masked by the, necessarily rather large, experimental uncertainty. The friction factors, however, show a considerable increase with increasing wall-to-bulk temperature ratio. This effect is significantly underestimated by Deissler's and Sze's analyses. The analysis by Davenport and Leppert is in better agreement with the experimental results but their predictions contain an element of arbitrariness because both the magnitude and the distribution of the radial velocities are postulated rather than found by solution of the equations of motion.

The reason for the discrepancies between the analyses and the experimental data—with the exception of the study by Koppel and Smith which, however, is of limited interest in the present context due to the peculiar behavior of both the thermodynamic and the transport properties in the vicinity of the critical point—clearly is that they are based on oversimplifying assumptions. On the other hand, if analytical or semi-analytical solutions are to be obtained rather gross simplications are necessary due to the nonlinearity of the governing equations and the strong coupling between them. Therefore, if more accurate results are desired resort must be made to finite-difference methods. In this way the basic equations may be integrated with a minimum of simplifying assumptions and, furthermore, the effect of the approximations made may be estimated from the numerical solutions.

In the present study an implicit finite-difference scheme is developed for numerical integration of the basic (boundary-layer) equations. For the case of fully developed flow at the start of the heated section examples are computed for uniform heat flux at the wall and for uniform wall temperature.

BASIC EQUATIONS

In the formulation of the present problem all the usual boundary-layer approximations were made. This is common practice for incompressible flow even though, for flow in long ducts, the lack of similarity between velocity and temperature profiles, respectively, at different axial locations makes it impossible to provide axially independent estimates of the order of magnitude of the individual terms in the complete equations. The agreement between predictions based on solutions of the boundary-layer equations and experimental results has, so far, provided the justification for applying the approximations. However, recently a solution of the complete equations for incompressible flow in the inlet region of a plane duct has been presented by Wang and Longwell [8]. Comparison of their results with the previous analytical solution by Schlichting [9], improved by Collins and Schowalter [10, 11], and with the finite-difference solution by Bodoia and Osterle [12] indicates that with the usual restriction to Reynolds numbers, based on the distance from the inlet, above a certain value the boundary-layer approximations are indeed valid for flow in ducts. In order to obtain the same degree of approximation as for external flow the minimum Reynolds number must, however, be higher than the usually accepted value of some two hundred.

As for the energy equation the crucial assumption is that the molecular contribution to axial thermal energy transfer may be neglected. For flow with constant properties the validity of this assumption, for Péclet numbers above 100–200, has been confirmed by the eigenvalue solution by Singh [13] and the approximate solutions, for Prandtl numbers in the liquid metals range, by Schneider [14] and Petukhov and Tsvetkov [15]. With the close analogy that exists between momentum and thermal energy transfer for fluids with Prandtl numbers close to unity this result also indicates that for flow of gases the molecular contribution to axial momentum transfer may be neglected.

In the present case we have the additional complication of the property variation. It is hardly conceivable that the perturbation caused by the latter should change the order of magnitude of otherwise second-order terms in the equations. However, a definite answer to this question can be obtained only *a posteriori* by estimating, from the numerical solutions, the magnitude of the neglected terms.

If we restrict our considerations to axially

symmetric flows—which implies that when natural convection effects are significant only flow in vertical tubes will be considered—and a cylindrical coordinate system is chosen with the x-axis positive upwards the boundary-layer equations become

$$\rho u \frac{\partial u}{\partial x} + \rho v \frac{\partial u}{\partial r} = -g\rho - \frac{\mathrm{d}p}{\mathrm{d}x} + \frac{1}{r}\frac{\partial}{\partial r}\left(r\mu \frac{\partial u}{\partial r}\right) \quad (1)$$

$$\frac{\partial}{\partial x}(\rho u) + \frac{1}{r}\frac{\partial}{\partial r}(r\rho v) = 0 \quad (2)$$

$$\rho u \frac{\partial H}{\partial x} + \rho v \frac{\partial H}{\partial r} = u \frac{\mathrm{d}p}{\mathrm{d}x} + \frac{1}{r}\frac{\partial}{\partial r}\left(r \frac{k}{c_p}\frac{\partial H}{\partial r}\right) + \mu\left(\frac{\partial u}{\partial r}\right)^2 \quad (3)$$

In addition to these equations we need equations of state to give the necessary relations between the thermodynamic properties and expressions for the temperature dependence of the transport coefficients (assuming that the latter are independent of pressure). The assumption will be made that the gas obeys the perfect gas law

$$p = \rho RT \quad (4)$$

This holds to a good approximation as long as the gas is not too dense.

With the enthalpy at $x = 0$ as reference value we have

$$H - H_0 = \int_{T_0}^{T} c_p \,\mathrm{d}T \quad (5)$$

For the monatomic gases the specific heat and the Prandtl number do not vary significantly with temperature. However, for diatomic and polyatomic gases the variation of the specific heat, although less than that of the transport coefficients, is not negligible. For all three properties the dependence will be taken as power laws which give reasonably good approximations to the actual behavior,

$$c_p/c_{p,0} = (T/T_0)^a \quad (6)$$

$$\mu/\mu_0 = (T/T_0)^b \quad (7)$$

$$k/k_0 = (T/T_0)^c \quad (8)$$

At the wall the no-slip condition, the impermeability of the wall, and the imposed thermal condition give the following boundary conditions,

$$\left.\begin{aligned} &u = 0; \quad v = 0; \\ &H = H(T_w) \text{ for specified wall temperature;} \\ &\frac{\partial H}{\partial r} = \frac{k_w}{c_{p,w}} q_w'' \text{ for specified heat flux.} \end{aligned}\right\} \quad (9)$$

At the centerline the following conditions arise from the symmetry of the problem,

$$\frac{\partial u}{\partial r} = 0; \quad v = 0; \quad \frac{\partial H}{\partial r} = 0 \quad (10)$$

For $x = 0$ we have the starting conditions

$$u = 2u_0[1 - (r/r_0)^2]; \; v = 0; \; H = H_0 \quad (11)$$

Strictly, the starting profile is parabolic only if expansion work and viscous dissipation are negligible, i.e. if the Mach number at the inlet is sufficiently small. For cases with appreciable heating this condition is already imposed because the Mach number at the exit must be below unity.

When non-dimensional variables are substituted in the foregoing equations one obtains,

$$\left.\begin{aligned} &\rho^+ u^+ \frac{\partial u^+}{\partial x^+} + \rho^+ v^+ \frac{\partial u^+}{\partial r^+} = \\ &\quad -\tfrac{1}{2}\frac{N_{Gr^*,0}\, N_{Pr,0}}{N_{Re,0}}\rho^+ + \frac{\mathrm{d}P}{\mathrm{d}x^+} \\ &\quad + 2N_{Pr,0}\frac{1}{r^+}\frac{\partial}{\partial r^+}\left(r^+\mu^+\frac{\partial u^+}{\partial r^+}\right) \end{aligned}\right\} \quad (12)$$

$$\frac{\partial}{\partial x^+}(\rho^+ u^+) + \frac{1}{r^+}\frac{\partial}{\partial r^+}(r^+\rho^+ v^+) = 0 \quad (13)$$

$$\left.\begin{aligned} &\rho^+ u^+ \frac{\partial H^+}{\partial x^+} + \rho^+ v^+ \frac{\partial H^+}{\partial r^+} = \\ &\quad \frac{2}{r^+}\frac{\partial}{\partial r^+}\left(r^+\frac{k^+}{c_p^+}\frac{\partial H^+}{\partial r^+}\right) \\ &\quad -(\gamma_0 - 1)M_0^2\left[u^+\frac{\mathrm{d}P}{\mathrm{d}x^+} - 2N_{Pr,0}\mu^2\left(\frac{\partial u^+}{\partial r^+}\right)^2\right] \end{aligned}\right\} \quad (14)$$

$$H^+ = \int_1^{\theta} c_p^+ \, \mathrm{d}\theta = \frac{1}{1+a}(\theta^{1+a} - 1) \tag{15}$$

$$\rho^+ = p^+/\theta \tag{16}$$

$$c_p^+ = \theta^a \tag{17}$$

$$\mu^+ = \theta^b \tag{18}$$

$$k^+ = \theta^c \tag{19}$$

The boundary conditions are

$$\left.\begin{aligned} &r^+ = 1;\ x^+ > 0: \\ &\quad u^+ = 0; \quad v^+ = 0 \\ &\quad H^+ = H^+(\theta_w), \quad \text{or} \quad \frac{\partial H^+}{\partial r^+} = \frac{c_p^+}{k^+} q^+ \end{aligned}\right\} \tag{20}$$

$$r^+ = 0; \quad x^+ > 0: \quad \frac{\partial u^+}{\partial r^+} = 0; \quad v^+ = 0; \quad \frac{\partial H^+}{\partial r^+} = 0 \tag{21}$$

$$x^+ = 0; \quad 0 \leqslant r^+ \leqslant 1: \quad u^+ = 2(1 - r^{+2}); \quad v^+ = 0; \quad H^+ = 0 \tag{22}$$

Heat-transfer results are expressed in terms of the conventional Nusselt number, based on the difference between the wall temperature and the mixed mean temperature of the gas. As a reference temperature for evaluation of the physical properties in the Nusselt number and the Reynolds number the mixed mean temperature was chosen. In terms of the non-dimensional variables the Nusselt number becomes

$$N_{Nu,m} = \frac{2q^+}{k_m^+(\theta_w - \theta_m)} \tag{23}$$

where, for specified wall temperature, the wall heat flux is

$$q^+ = \left(\frac{k^+}{c_p^+}\frac{\partial H^+}{\partial r^+}\right)_{r^+=1} \tag{24}$$

The mixed mean temperature is taken as the temperature corresponding to the mixed mean enthalpy,

$$H_m^+ = \frac{\int_0^1 \rho^+ u^+ H^+ r^+ \, \mathrm{d}r^+}{\int_0^1 \rho^+ u^+ r^+ \, \mathrm{d}r^+} = 2\int_0^1 \rho^+ u^+ H^+ r^+ \, \mathrm{d}r^+ \tag{25}$$

The friction factor is defined as†

$$f = \frac{\tau_w}{\frac{1}{2}(\rho u)_m u_m} \tag{26}$$

or, in terms of non-dimensional variables,

$$f N_{Re,m} = \frac{2\tau_w^+}{\mu_m^+ \int_0^1 u^+ r^+ \, \mathrm{d}r^+} \tag{27}$$

where

$$\tau_w^+ = -\left(\mu^+ \frac{\partial u^+}{\partial r^+}\right)_{r^+=1} \tag{28}$$

With the governing equations written in non-dimensional form we may identify the independent parameters in the problem. For reference purposes it will be convenient to divide them into two groups, "operational" and "property" parameters. Of operational parameters we find $(\gamma - 1)M^2$, N_{Gr^*}/N_{Re} (or $N_{Gr^*} N_{Pr}/N_{Re}$), and either q^+ or θ_w; the property parameters are the Prandtl number and the three exponents of the power laws. The latter which appear as independent in a mathematical sense are of course not physically independent; they simply specify a particular gas and a certain temperature range for which the solutions will be valid. Neither are the operational parameters completely independent. The natural convection and the dissipation parameters are coupled through, e.g. the Reynolds number and the diameter of the tube which, although they do not appear explicitly, impose certain restrictions on the relative magnitude of the two parameters. For a perfect gas with pressure-independent viscosity the connection between these parameters is particularly simple since, for fixed gas temperature, $M \propto N_{Re}/(pD)$ and $N_{Gr^*} \propto p^2 D^3$. These relations are shown on Fig. 1 for air at 80°F.

For sufficiently small values of N_{Gr^*}/N_{Re} (below 20, say) natural convection effects will

† There are, in fact, two other ways of defining the friction factor, namely,

$$f = \frac{\tau_w}{\frac{1}{2}(\rho u)_m^2/\rho_m}, \quad \text{and} \quad f = \frac{\tau_w}{\frac{1}{2}\rho_m u_m^2}$$

The former of the two definitions is the one usually employed in the reduction of experimental pressure drop data where the flow is treated as one-dimensional. It can be shown that all three definitions are equivalent for perfect gases with constant specific heats if the somewhat arbitrary definition $\rho_m = \rho(\theta_m)$ is introduced.

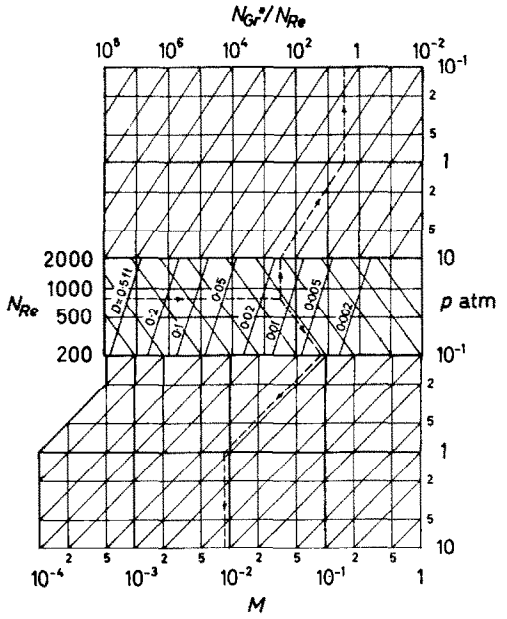

FIG. 1. Relation between the Mach number and the natural convection parameter for flow of air in circular tubes at 80°F.

be negligible. On the other hand, when the Mach number is less than approximately 0·1 both expansion work and viscous dissipation are insignificant. From Fig. 1 it is seen that the two effects are mutually exclusive and that, in a limited range, both may be neglected.

If a comparison is made with constant-properties flow (including buoyancy effects) one finds that our operational parameters have their exact counterparts, with the exception of the parameter related to the thermal boundary condition. To N_{Gr}^*/N_{Re} corresponds N_{Gr}/N_{Re}, and to $(\gamma - 1)M^2$ corresponds the Eckert number, $u_m^2/(c_p \Delta T)$. The increased complexity due to the variation of the properties shows up in the property parameters and in the parameter related to the thermal boundary condition. The latter indicates the nonlinearity of the energy equation which means that solutions cannot be superimposed.

FINITE-DIFFERENCE SCHEME

For the numerical integration a two-level scheme with central differences in the radial direction was chosen. The designation of mesh points is shown on Fig. 2. Introducing a central difference operator

$$\delta_{m,n} = \phi_{m,n+1} - \phi_{m,n-1}$$

$$\delta^2_{m,n} = \phi_{m,n+1} - 2\phi_{m,n} + \phi_{m,n-1}$$

and a weighting parameter σ, $0 \leqslant \sigma \leqslant 1$, we can express the difference quotients by Taylor

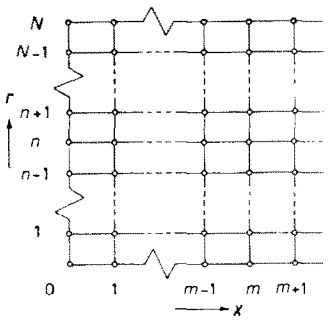

FIG. 2. Designation of mesh points.

series expansions about the point $[(m + \sigma)\Delta x, n\Delta r]$,

$$\frac{\partial \phi}{\partial x} = \frac{\phi_{m+1,n} - \phi_{m,n}}{\Delta x} - \tfrac{1}{2}(1 - 2\sigma)\frac{\partial^2 \phi}{\partial x^2}\Delta x + 0(\Delta x^2) \qquad (29)$$

$$\frac{\partial \phi}{\partial r} = \frac{\sigma \delta \phi_{m+1,n} + (1 - \sigma)\,\delta \phi_{m,n}}{2\Delta r} + 0(\Delta x^2) + 0(\Delta r^2) \qquad (30)$$

$$\frac{\delta^2 \phi}{\partial r^2} = \frac{\sigma \delta^2 \phi_{m+1,n} + (1 - \sigma)\,\delta^2 \phi_{m,n}}{\Delta r^2} + 0(\Delta x^2) + 0(\Delta r^2) \qquad (31)$$

When the three equations (12)–(14) are written in expanded form, the power laws (17)–(19) are introduced, and the derivatives are replaced by difference quotients according to (29)–(31), a set of algebraic equations is obtained. From these equations, supplemented with the boundary conditions (20) and (21) and with the thermodynamic relations (15) and (16), the unknown values of u^+, v^+, H^+, and P on the $(m + 1)$th line may be solved for when the corresponding values on the preceding line are known. Due to the parabolic nature of the boundary-layer equations (as contrasted to the elliptic nature

of the complete equations) the entire flow and enthalpy fields may thus be found by stepping ahead in the axial direction, starting at $x^+ = 0$ with the initial values (22).

When σ is zero the finite-difference scheme is explicit, so called because the unknowns in the difference equations may be solved for directly at each mesh point. For all other values of σ we have an implicit scheme and the unknowns must be found by solving the set of $3 \times N$ simultaneous equations that results when the difference equations are written for all interior points on the $(m + 1)$th line. Preliminary considerations showed that for an explicit scheme to be stable the axial step-width could at most be of the order of 10^{-4}. Since solutions up to $x^+ = 0{\cdot}2$–$0{\cdot}5$ were desired the number of steps in the axial direction would become of the order of several thousands, a nearly prohibitive magnitude. It was, therefore, decided to use an implicit method for which the axial step-width could be selected solely from convergence considerations.

For simple linear equations of the parabolic type as, e.g. the one-dimensional diffusion equation, it is known that a two-level scheme with $\sigma \geqslant \frac{1}{2}$ is unconditionally stable. Flügge-Lotz and Blottner [16] have shown that this is also true for the equations describing external compressible boundary-layer flow. A scheme with $\sigma = \frac{1}{2}$ (the Crank–Nicolson scheme) is particularly attractive because, as may be seen from equation (29), for this value of σ the truncation error is $0(\Delta x^2) + 0(\Delta r^2)$ whereas for all other values of σ the error is $0(\Delta x) + 0(\Delta r^2)$. However, for the present case the Crank–Nicolson scheme turned out not to be stable. The same result was found by Abbott in a study of axially symmetric incompressible flows in a tube [17].† In order to keep the truncation error as small as possible the value of σ should be chosen as close to one half as compatible with the stability requirement, The difference equations and the corresponding computer program was therefore formulated such that an arbitrary value could be assigned to σ. Preliminary computations indicated that a reasonable compromise between the stability requirement on one side and the rate of convergence of the solutions on the other could be obtained with $\sigma = \frac{3}{4}$.

In principle both the nonlinearity of the differential equations and the coupling between them carry over to the difference equations. However, one of the main advantages of finite-difference methods is that the difference equations may be linearized and uncoupled locally. The adverse effect of such linearization and of the uncoupling may, furthermore, be reduced *ad libitum* by iteration at each step.

In the momentum equation and in the energy equation the radial velocity appears only in the second convective term. If this term is linearized by introduction of the known value of $\rho^+ v^+$ from the preceding step, the continuity equation becomes completely uncoupled from the two former equations, and the solution of it may be deferred until the axial velocities and the enthalpies have been found. Because the flow is confined one must, however, introduce in the solution of the momentum equation the constraint that the total mass flow be conserved. This is done by including in the solution of the N difference equations derived from the momentum equation the integrated continuity equation. Since adding this equation does not in itself introduce any new unknown the pressure defect is included as an unknown in order to prevent overdetermination of the system of equations.‡

† The explanation proposed in reference 17 for the lack of stability of the Crank–Nicolson scheme must, however, be rejected. The instability does not, as suggested by Abbott, originate in the solution of the momentum equation *per se*. Both the result of an approximate stability analysis for flow in tubes [18] and some observations by Flügge–Lotz and Blottner [16] strongly indicate that the instability arises through the alternate propagation of errors by the momentum equation and the continuity equation, and that the amplification of errors mainly occurs in the solution of the latter.

‡ We are here in the paradoxical situation that we solve for three unknowns, u, v, and P (leaving, for the moment, the property variation out of the question), by means of only two independent equations. For external boundary layers this problem does not arise because the pressure is determined by the external (potential) flow. Wendel and Whitaker [19] comment on this paradox in connection with the finite-difference solution of the development of incompressible flow in a plane duct by Bodoia and Osterle [12]. The explanation must be sought in the fact that for confined flows the pressure variation is determined by the viscous flow field itself, but, since we have assumed that the pressure is uniform over the

Continued on next page

The linearization of the (expanded) momentum and energy equations further implies that known values are introduced for $\rho^+ u^+$ as well as for μ^+ and k^+/c_p^+. In the momentum equation only the term containing the derivative of the viscosity may be linearized in such a way as to furnish a direct coupling to the energy equation. Since the equally strong couplings through the viscosity itself and through the density had to be sacrificed anyway, it was decided to solve the two equations independently and to use iteration.

The sequence in which the computations were carried out at each axial step is, briefly stated, as follows: First the difference equations for H^+ were solved. Then the new value of P was determined and the difference equations for u^+ were solved. Finally the new values of $\rho^+ v^+$ were found from the continuity equation. Single iteration was used except where the number of mesh points in the radial direction was changed. Since this change seemed to introduce some instability three iterations were used at such points. At each axial step the computations started with known values from the preceding step in the linearized terms. However, as soon as new values became available weighted averages

$$\phi_{m+\sigma,n} = \sigma\phi_{m+1,n} + (1 - \sigma)\phi_{m,n}$$

and the corresponding difference quotients were substituted into the linearized terms.

The fact that the governing equations (12), (13), and (14) express the momentum balance and the conservation of mass and thermal energy, respectively, was utilized to keep a current check on the convergence of the numerical solutions. Using at $x^+ = 0$ the initial conditions (22) and at an arbitrary location average values obtained by integration over the cross-section one may, for each of the conserved quantities, make a control volume balance. In mathematical formulation this procedure amounts to a double integration, first with respect to r^+ (after multiplication by $2r^+$) and then with respect to x^+. A comparison of the values obtained from the right-hand side and from the left-hand side, respectively, will then show to which degree the solution is consistent with the basic equations.

The double integration yields the following three equations:

$$2\int_0^1 \rho^+ u^+ r^+ \,\mathrm{d}r^+ - 1 = 0 \tag{32}$$

$$2\int_0^1 \rho^+ u^{+2} r^+ \,\mathrm{d}r^+ - \tfrac{4}{3} = P - 4\,N_{Pr,0} \int_0^{x^+} \tau_w^+ \,\mathrm{d}x^+ - N_G \int_0^{x^+}\int_0^1 \rho^+ r^+ \,\mathrm{d}r^+ \,dx^+ \tag{33}$$

$$2\int_0^1 \rho^+ u^+ H^+ r^+ \,\mathrm{d}r^+ = 4\int_0^{x^+} q^+ \,\mathrm{d}x^+ - 2N_E \left[\int_0^{x^+} \frac{\mathrm{d}P}{\mathrm{d}x^+} \int_0^1 u^+ r^+ \,\mathrm{d}r^+ \,\mathrm{d}x^+ - 2\,N_{Pr,0} \int_0^{x^+}\int_0^1 \mu^+ \left(\frac{\partial u^+}{\partial r^+}\right)^2 r^+ \,\mathrm{d}r^+ \,\mathrm{d}x^+ \right] \tag{34}$$

In the numerical computations the integrations with respect to x^+ were performed with the trapezoidal formula which has a truncation error of $0(\Delta x^3)$, i.e. two orders of magnitude smaller than the truncation error of the finite-difference scheme. The radial integrations were carried out by means of Simpson's rule, giving an error of $0(\Delta r^5)$.

Satisfactory convergence of the solutions in the downstream region ($x^+ > 0{\cdot}05$) could be obtained with twenty mesh points in the radial direction and an axial step-width of $\Delta x^+ = 10^{-3}$. Due to the discontinuity in the thermal boundary condition at $x^+ = 0$ the discrepancies, particularly in the thermal energy balance, tended to be rather large in the first few steps. The computations were therefore started with $N = 80$ and $\Delta x^+ = 1{\cdot}25 \times 10^{-4}$. At three preassigned locations the axial step-width was doubled and at the first two the number of mesh points in the radial direction were halved. For the same reason the solutions are in the following considered only for $x^+ \geqslant 10^{-3}$.

The problem was coded in ALGOL and solved on the CDC 1604A computer of A/S

cross-section, it can depend directly on the axial velocities only. The pressure is, therefore, not a true variable in the same sense as the velocity components are, and the necessary, third, relation may be found from either of the two equations simply by eliminating the radial velocity component.

Regnecentralen (The Danish Computation Center). The computation time for integration up to $x^+ = 0{\cdot}5$ was about 10 min; this corresponds to approximately one second per axial step with twenty mesh points, including one iteration.

NUMERICAL RESULTS

In the numerical examples the emphasis has been placed on solutions for uniform heat flux at the wall. The inlet Mach numbers were chosen such that expansion work and viscous dissipation were almost negligible throughout the tube. The corresponding terms are, however, included in the computer program, and it is the intention in the future to extend the solutions to cases with high Mach numbers in the downstream region. All examples were computed with properties corresponding to those of air,

$$N_{Pr,0} = 0{\cdot}72; \quad \gamma_0 = 1{\cdot}40; \quad a = 0{\cdot}12; \quad b = 0{\cdot}67; \quad c = 0{\cdot}71.$$

Uniform heat flux

Local wall parameters from a series of five solutions with increasing heat flux at the wall are given in Table 1. The Mach number at the inlet was in all cases 0·01 and the natural convection parameter, $N_{Gr^*,0}/N_{Re,0}$, was unity, a value for which natural convection effects are negligible. For the two lowest heat fluxes the integration was continued until $x^+ = 0{\cdot}5$ where, for flow with constant fluid properties, the temperature profile would differ insignificantly from the fully developed profile. At higher heat fluxes the computations were not carried so far because of the rapid increase of the gas temperature; with power laws for the transport coefficients and the specific heat it would be unrealistic to let θ exceed values of some 6–8.

The local Nusselt numbers are plotted on Fig. 3. They show surprisingly small deviations from the solution for constant fluid properties; even at the highest heat flux, resulting in a maximum wall-to-bulk temperature ratio of more than three, the deviations are at most some twenty per cent. This result is, however, consistent with the fact that in experimental investigations with heat fluxes corresponding to values of q^+ up to 10, deviations from the

Table 1. Wall parameters for pure forced convection with uniform heat flux ($N_{Gr,0}/N_{Re,0} = 1$; $M_0 = 10^{-2}$)

x^+	$N_{Nu,m}$	θ_w	$fN_{Re,m}$	T_w/T_m
		$q^+ = 0{\cdot}5$		
0·001	16·36	1·063	16·92	1·061
0·002	12·86	1·081	17·17	1·077
0·005	9·48	1·115	17·58	1·104
0·01	7·62	1·149	17·94	1·127
0·02	6·24	1·196	18·30	1·150
0·05	4·99	1·286	18·58	1·170
0·1	4·48	1·394	18·43	1·164
0·2	4·32	1·574	17·89	1·132
0·5	4·34	2·098	17·02	1·073
		$q^+ = 2$		
0·001	16·73	1·246	19·65	1·236
0·002	13·21	1·315	20·60	1·295
0·005	9·77	1·438	22·07	1·383
0·01	7·84	1·563	23·16	1·448
0·02	6·34	1·727	23·88	1·491
0·05	4·92	2·034	23·32	1·462
0·1	4·35	2·383	21·31	1·347
0·2	4·27	2·988	18·80	1·196
0·5	4·34	4·88	16·92	1·067
		$q^+ = 5$		
0·001	17·36	1·588	24·98	1·557
0·002	13·77	1·746	27·12	1·680
0·005	10·16	2·020	29·97	1·837
0·01	8·04	2·292	31·4	1·914
0·02	6·33	2·641	31·1	1·898
0·05	4·72	3·27	27·03	1·673
0·1	4·20	3·99	22·09	1·395
0·2	4·27	5·36	18·40	1·174
		$q^+ = 10$		
0·001	18·19	2·109	33·5	2·029
0·002	14·41	2·394	37·0	2·216
0·005	10·48	2·876	40·6	2·399
0·01	8·09	3·35	40·7	2·402
0·02	6·15	3·94	37·2	2·221
0·05	4·47	4·98	28·39	1·742
0·1	4·14	6·21	21·40	1·359
		$q^+ = 20$		
0·001	19·31	3·04	49·1	2·813
0·002	15·15	3·54	53·7	3·04
0·005	10·64	4·36	55·2	3·12
0·01	7·88	5·15	50·6	2·896
0·02	5·77	6·12	41·5	2·435
0·05	4·21	7·80	27·81	1·703

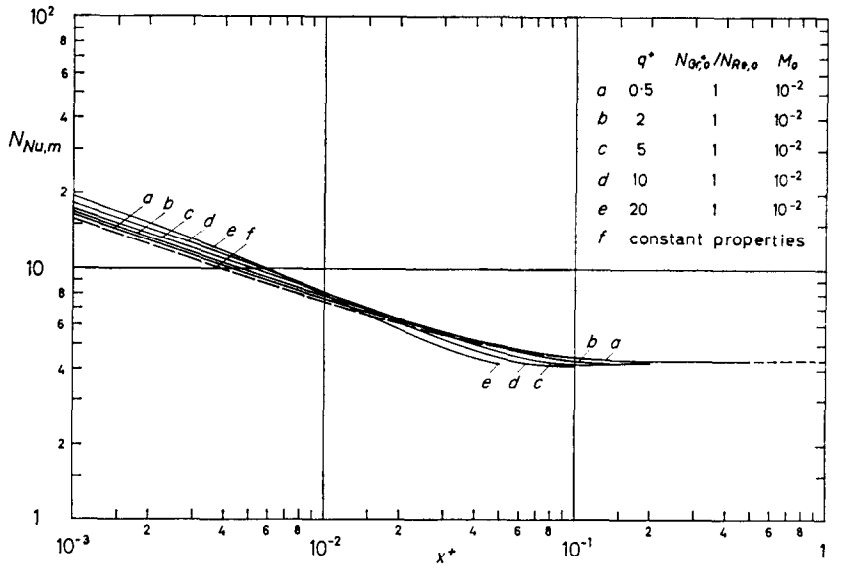

FIG. 3. Local Nusselt numbers for pure forced convection with uniform heat flux.

constant-properties solution could hardly be detected.

Surprising also is the fact that for small values of x^+ the Nusselt number increases with increasing heat flux, contrary to the predictions of previous analyses. The explanation of this unexpected behavior lies in the perturbation of the flow field. On Figs. 4 and 5 the development of the axial and radial velocities is shown for $q^+ = 5$ and $q^+ = 20$. One notes that the effect of the property variation on the axial velocity profile is the opposite of what has been common belief: instead of a sharpening of the peak one finds a flattening of the profile. In the light of the information contained in the figures both the relatively small magnitude and the direction of the deviations of the Nusselt numbers from the constant-properties solution become understandable. We are clearly dealing with several, partly opposing, effects: the increase of the thermal conductivity near the wall increases the radial conduction; the larger velocity gradients at the wall tend to increase the axial convection but the decrease of the density acts in the opposite direction; finally we have the radial convection which in the beginning adds to the heat transfer from the wall but later is reversed.

It is interesting to note that "overshoot" profiles may occur at high heating rates since, for flow in ducts, such profiles are usually associated with superimposed natural convection. That in this case the overshoot did not arise from buoyancy effects was checked by repeating the computations for $q^+ = 20$ with the sign of the gravitational term reversed (corresponding to downward flow); this changed the axial velocities by less than 0·1 per cent. It should be noted that velocity profiles with the same trends as the present—even with overshoot—were predicted by the approximate analysis by Davenport and Leppert [3].

The development of the temperature profiles is shown on Fig. 6. One sees that there is a qualitative agreement between the profile calculated by Deissler [1] and the profile from the present solution for $q^+ = 20$ at $x^+ = 0{\cdot}05$.†

On Fig. 7 local friction factors are plotted together with the wall-to-bulk temperature ratio. In contrast to the Nusselt numbers the friction factors show a considerable increase over the value for isothermal flow. One also notes that the axial variation of $fN_{Re,m}$ exhibits a striking similarity to the variation of the temperature ratio.

† At $x^+ = 0{\cdot}05$ the wall-to-bulk temperature ratio happens to be 1·70, the same value for which Deissler shows a temperature profile.

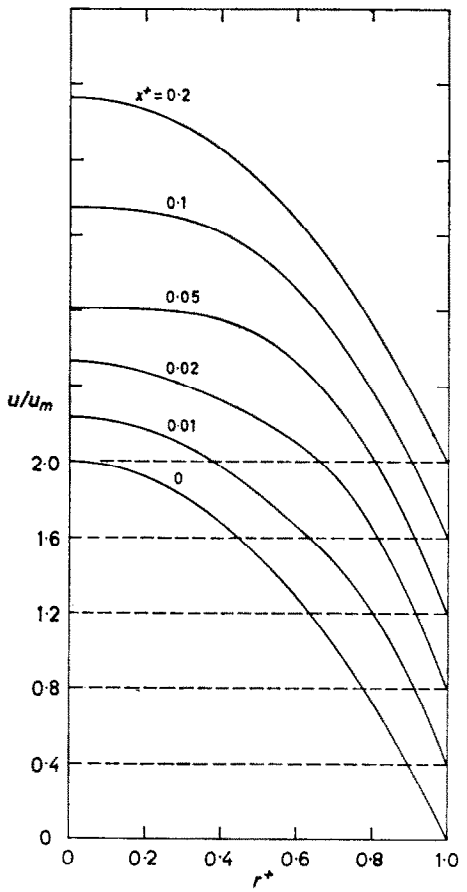

FIG. 4a. Axial velocity profiles for pure forced convection with uniform heat flux; $q^+ = 5$.

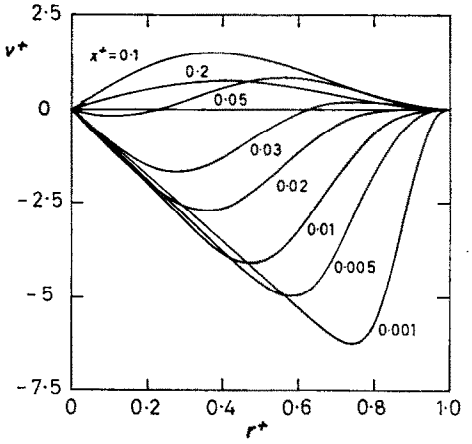

FIG. 4b. Radial velocity profiles for pure forced convection with uniform heat flux; $q^+ = 5$.

An important general conclusion that may be drawn from Figs. 3 and 7 is the fact that—irrespective of the heating rate—significant variations of the fluid properties and, hence, effects of the latter on heat transfer and wall friction, are limited to the usual thermal entrance region. In fact, the higher the flux is, the more rapidly both the Nusselt number and the friction factor approach the asymptotic values for constant-properties flow.

Effect of superimposed natural convection

In order to study the effect of superimposed natural convection computations were carried out for values of $N_{Gr^*,0}/N_{Re,0}$ of 10, 10^2, and 10^3 and a moderate heat flux, $q^+ = 5$. Only the case where the flow was in the same direction as the

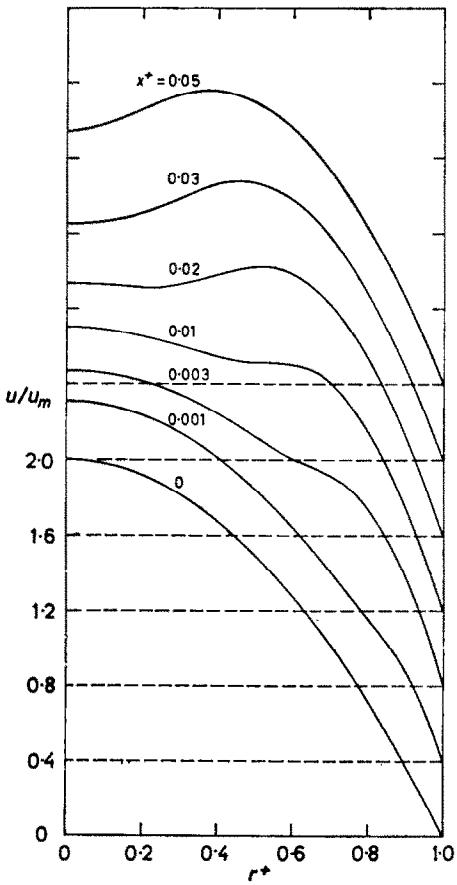

FIG. 5a. Axial velocity profiles for pure forced convection with uniform heat flux; $q^+ = 20$.

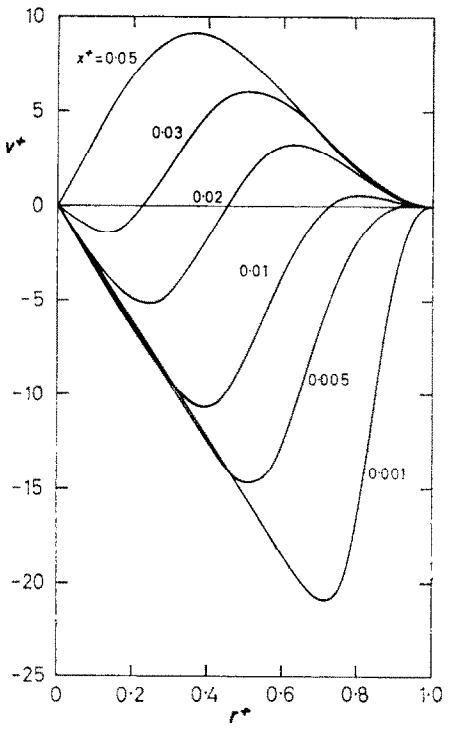

FIG. 5b. Radial velocity profiles for pure forced convection with uniform heat flux; $q^+ = 20$.

buoyancy forces, i.e. upward flow, was considered. This is the situation usually encountered in applications and, moreover, it is known [20, 21] that when the buoyancy forces act against the flow instability tends to develop at quite low values of the natural convection parameter and transition to turbulent flow occurs at Reynolds numbers far below the usual critical value.

The wall parameters for $N_{Gr^*,0}/N_{Re,0} = 10^2$ and 10^3 are given in Table 2 and the local Nusselt numbers and friction factors are shown on Figs. 8 and 9 together with the solution for $N_{Gr^*,0}/N_{Re,0} = 1$.† One sees that superimposed natural convection, just as high heating rates, affects the friction factor more than it affects the Nusselt number. While for

$$N_{Gr^*,0}/N_{Re,0} = 10^3$$

the latter increases by at most 25 per cent, $fN_{Re,m}$ goes up by as much as 75 per cent.

The solutions again indicate that for laminar flow of gases at high heating rates significant variation of properties is largely limited to the usual thermal entrance region. This is also evident from the development of the axial velocity profile, shown on Fig. 10. Even though the characteristic overshoot with a considerable depression of the centerline velocity occurs, the profile at $x^+ = 0{\cdot}2$ differs little from the usual parabolic profile. It is worth noting that the velocity profile with overshoot caused by buoyancy effects is accompanied by radial velocities quite different from those associated with the overshoot profile for high heating rates.

Although solutions have been obtained for one particular value of the wall heat flux only,

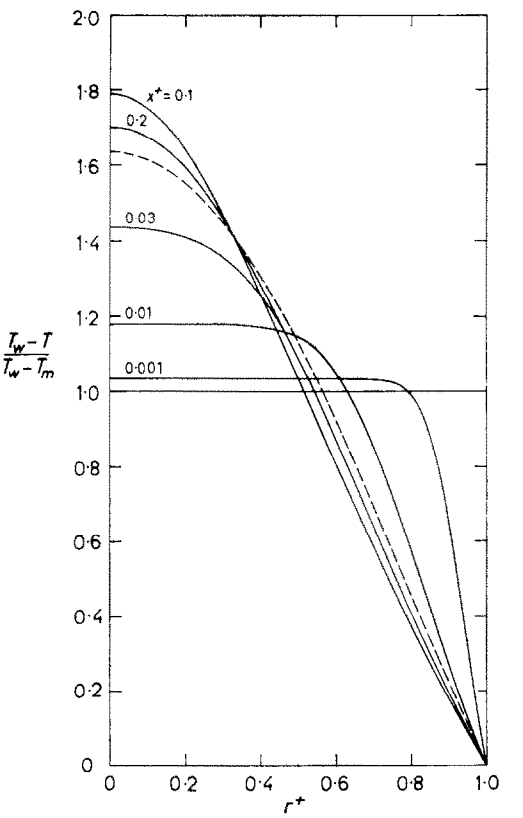

FIG. 6a. Temperature profiles for pure forced convection with uniform heat flux; $q^+ = 5$; ----- fully developed profile for constant properties.

† For $N_{Gr^*,0}/N_{Re,0} = 10$ the Nusselt number deviated less than 0·2 per cent and $fN_{Re,m}$ less than 0·7 per cent from the corresponding values for $N_{Gr^*,0}/N_{Re,0} = 1$.

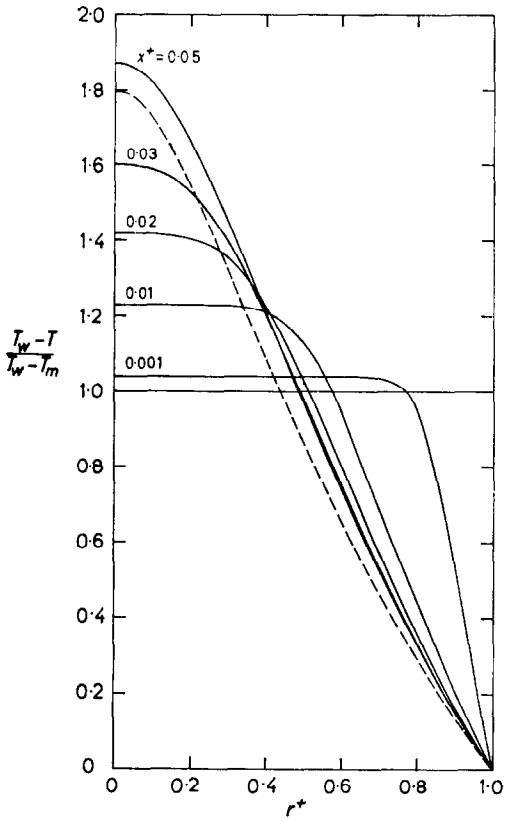

FIG. 6b. Temperature profiles for pure forced convection with uniform heat flux; $q^+ = 20$; - - - Deissler's profile [1].

we may from these solutions infer, tentatively, the limit beyond which buoyancy effects can no longer be neglected. Depending on the heating rate and on how large an error one is willing to accept the limiting value of $N_{Gr^*,0}/N_{Re,0}$ may

Table 2. Wall parameters for superimposed forced and natural convection with uniform heat flux ($q^+ = 5$)

$N_{Gr^*,0}/N_{Re,0} = 10^2$; $M_0 = 2 \times 10^{-2}$

x^+	$N_{Nu,m}$	θ_w	$fN_{Re,m}$	T_w/T_m
0·001	17·48	1·584	26·01	1·553
0·002	13·90	1·740	28·56	1·673
0·005	10·29	2·008	32·0	1·826
0·01	8·17	2·274	33·7	1·899
0·02	6·45	2·617	33·2	1·881
0·05	4·81	3·25	28·18	1·660
0·1	4·25	3·97	22·44	1·391
0·2	4·28	5·36	18·44	1·174

Table 2—continued

$N_{Gr^*,0}/N_{Re,0} = 10^3$; $M_0 = 10^{-3}$

x^+	$N_{Nu,m}$	θ_w	$fN_{Re,m}$	T_w/T_m
0·001	18·51	1·552	35·1	1·523
0·002	14·98	1·689	41·3	1·626
0·005	11·43	1·916	50·1	1·745
0·01	9·35	2·138	54·8	1·787
0·02	7·66	2·423	54·1	1·744
0·05	5·87	3·01	38·9	1·543
0·1	4·69	3·86	25·15	1·356
0·2	4·32	5·35	18·85	1·173

Table 3. Wall parameters for pure forced convection with uniform wall temperature ($N_{Gr^*,0}/N_{Re,0} = 1$; $M_0 = 10^{-2}$)

$\theta_w = 0·5$

x^+	$N_{Nu,m}$	q^+	$fN_{Re,m}$	T_w/T_m
0·001	11·98	−4·68	9·23	0·508
0·002	9·41	−3·58	9·31	0·514
0·005	6·90	−2·462	9·39	0·525
0·01	5·62	−1·853	9·62	0·540
0·02	4·69	−1·364	10·00	0·564
0·05	3·94	−0·853	10·91	0·619
0·1	3·71	−0·538	12·01	0·692
0·2	3·66	−0·268	13·40	0·800

$\theta_w = 2$

x^+	$N_{Nu,m}$	q^+	$fN_{Re,m}$	T_w/T_m
0·001	14·62	4·40	31·8	1·916
0·002	11·31	3·37	30·8	1·872
0·005	8·04	2·340	29·21	1·783
0·01	6·30	1·769	27·43	1·686
0·02	5·00	1·309	25·16	1·560
0·05	3·92	0·828	21·57	1·356
0·1	3·62	0·516	18·82	1·192
0·2	3·64	0·203	16·83	1·062

$\theta_w = 5$

x^+	$N_{Nu,m}$	q^+	$fN_{Re,m}$	T_w/T_m
0·001	16·06	35·3	80·1	4·00
0·002	12·04	27·31	69·3	3·65
0·005	8·13	19·37	55·4	3·07
0·01	6·04	14·80	44·9	2·579
0·02	4·59	11·11	35·1	2·082
0·05	3·61	7·09	24·32	1·502
0·1	3·58	3·80	18·55	1·180
0·15	3·64	1·735	16·88	1·068

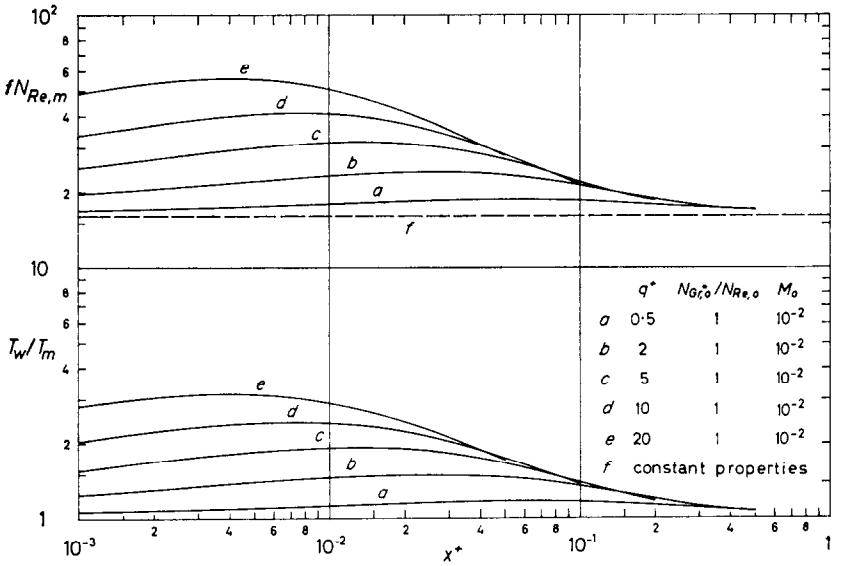

FIG. 7. Local friction factors and wall-to-bulk temperature ratios for pure forced convection with uniform heat flux.

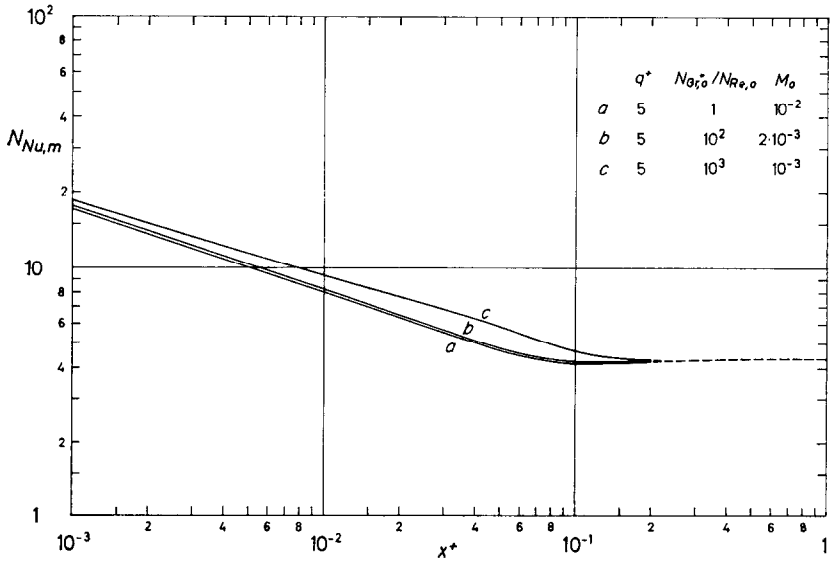

FIG. 8. Local Nusselt numbers for superimposed forced and natural convection with uniform heat flux.

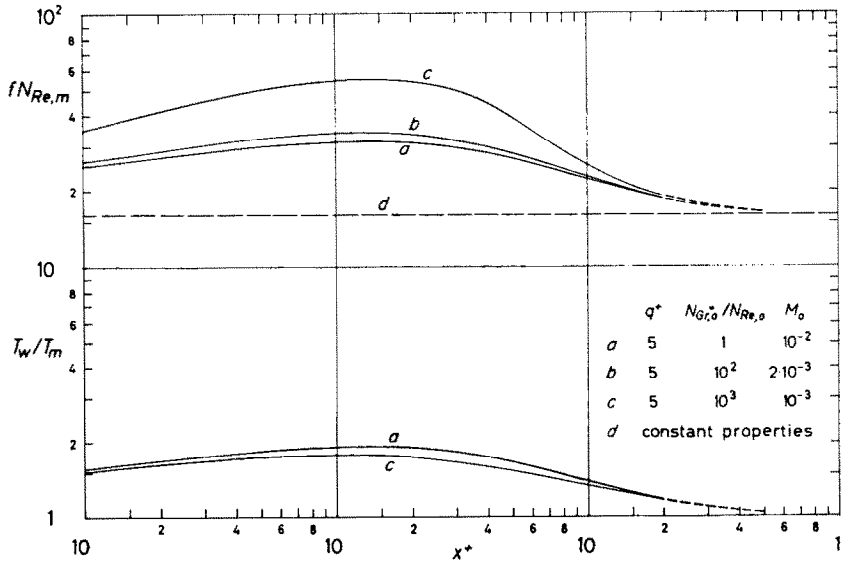

FIG. 9. Local friction factors and wall-to-bulk temperature ratios for superimposed forced and natural convection with uniform heat flux.

be chosen somewhere between 10 and 50. The latter value coincides with the limit for $N_{Gr,m}/N_{Re,m}$ proposed by Brown [21] for fully developed flow with constant properties.

Uniform wall temperature

Three cases with uniform wall temperature were computed, two with heating of the gas ($\theta_w = 2$ and 5) and one with cooling ($\theta_w = 0{\cdot}5$). Local wall parameters are given in Table 3; local values of the Nusselt number and the friction factor are plotted on Figs. 11 and 12, respectively. Both the Nusselt numbers and the friction factors are seen to follow the same pattern as was found for uniform heat flux. When the gas is cooled the effect of the property variation is reversed, as one would indeed expect.

On Fig. 13 axial velocity profiles and temperature profiles, respectively, for heating of the gas are compared with those obtained with cooling. One sees clearly that, as already noted for uniform heat flux, the distortion of the velocity profiles are exactly opposite of what has hitherto been believed. The temperature profiles, however, do show the expected effect of the property variation.

Limits on applicability of numerical solutions

The numerical solutions are, as mentioned previously, considered only for $x^+ \geqslant 10^{-3}$. In an Appendix it is shown that the errors introduced by applying the boundary layer approxinations are small as long as the Péclet number, based on the distance from the point where the heating starts, is above some 500. On Fig. 14 these limitations are shown in terms of x^+ and $N_{Pe,0}$.

The significance of the limitations may be appreciated more readily when expressed in terms of the length-to-diameter ratio:

$N_{Pe,0}$	200	1000	3000
$(x/D)_{\min}$	2·5	0·5	1·5

Clearly, neither the application of the boundary-layer approximations nor the relatively large initial error gives rise to any serious limitation of the applicability of the numerical solutions.

Empirical equations

For design purposes it may sometimes be more convenient to have the solutions expressed as equations rather than in graphical or tabular form. The following empirical expressions

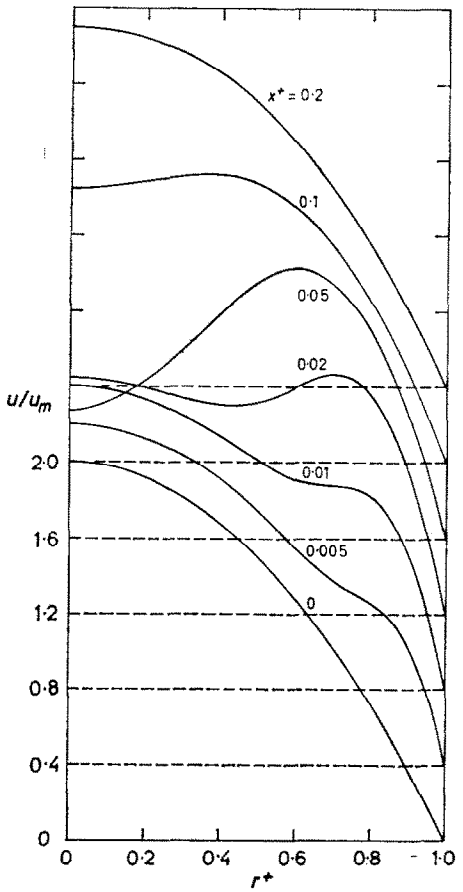

FIG. 10a. Axial velocity profiles for superimposed forced and natural convection with uniform heat flux; $q^+ = 5$.

represent the solutions for pure forced convection with a maximum error of ± 3 per cent.

Heat transfer

Uniform heat flux, $0 < q^+ < 10$:

$$N_{Nu,m} = 4{\cdot}36\,[1 - \exp(-17\,x^+)] + ax^{+-1/3}\exp(-bx^{+5/4}) \quad (35)$$

$$a = 1{\cdot}53 + 0{\cdot}11\,q^{+0{\cdot}4}$$

$$b = 20 + 5{\cdot}0\,\sqrt{q^+}$$

Uniform heat flux, $10 < q^+ < 20$:

$$N_{Nu,m} = 4{\cdot}36\,[1 - \exp(-17\,x^+)] + ax^{+-1/3}\exp(-bx^+) \quad (36)$$

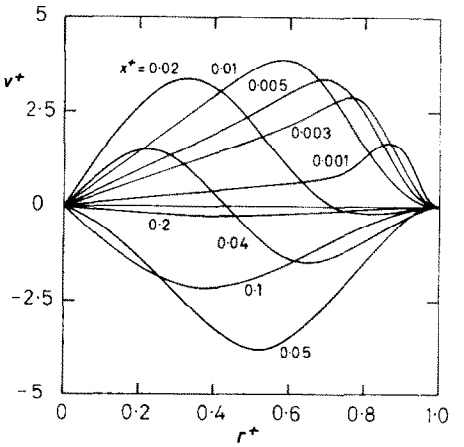

FIG. 10b. Radial velocity profiles for superimposed forced and natural convection with uniform heat flux; $q^+ = 5$.

$$a = 1{\cdot}74 + 0{\cdot}011\,q^+$$

$$b = 10 + 2{\cdot}7\,\sqrt{q^+}$$

Uniform wall temperature, $0{\cdot}5 < \theta_w < 2$:

$$N_{Nu,m} = 3{\cdot}66\,[1 - \exp(-13{\cdot}5\,x^+)] + ax^{+-1/3}\exp(-bx^+) \quad (37)$$

$$a = 1{\cdot}14 + 0{\cdot}155\theta_w$$

$$b = 8{\cdot}1 + 1{\cdot}95\theta_w$$

Wall friction

$$1 < T_w/T_b < 1{\cdot}5: \quad fN_{Re,m} = 16\,(T_w/T_b) \quad (38)$$

$$1{\cdot}5 < T_w/T_b < 3: \quad fN_{Re,m} = 15{\cdot}5\,(T_w/T_b)^{1{\cdot}10} \quad (39)$$

$$0{\cdot}5 < T_w/T_b < 1: \quad fN_{Re,m} = 16\,(T_w/T_b)^{0{\cdot}81} \quad (40)$$

Davenport and Leppert [3] found that their experimentally determined friction factors could be correlated by

$$fN_{Re,m} = 16\,(T_w/T_b)^{1{\cdot}35}$$

for temperature ratios up to a little over two. In view of the considerable difficulties both in obtaining accurate measurements of the pressure drop and in the subsequent evaluation of the wall shear stress from these measurements, the agreement with the present results must be considered good.

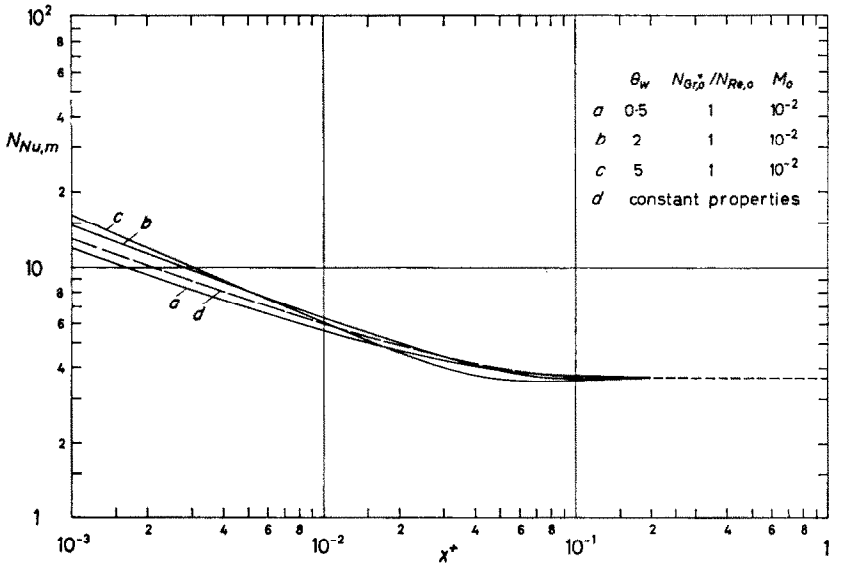

FIG. 11. Local Nusselt numbers for pure forced convection with uniform wall temperature.

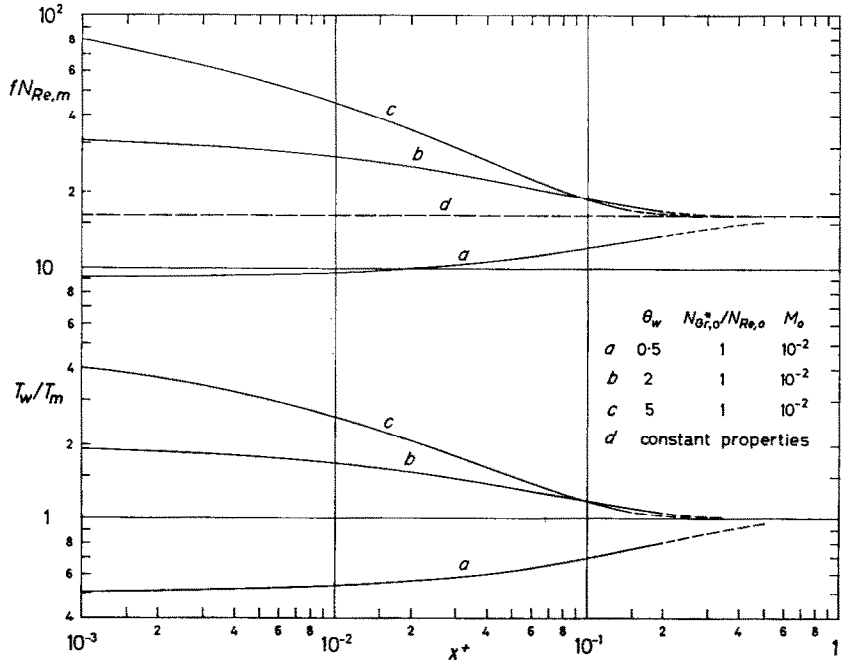

FIG. 12. Local friction factors and wall-to-bulk temperature ratios for pure forced convection with uniform wall temperature.

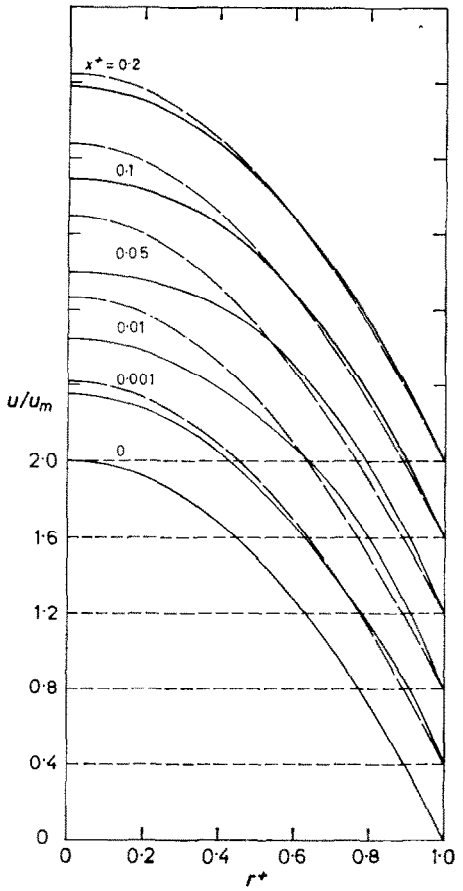

FIG. 13a. Axial velocity profiles for pure forced convection with uniform wall temperature; ——— $\theta_w = 2$; - - - - $\theta_w = 0{\cdot}5$.

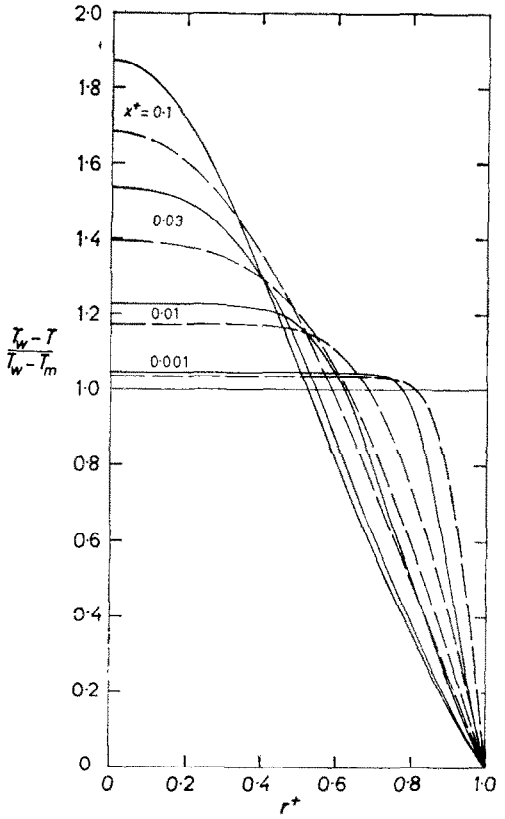

FIG. 13b. Temperature profiles for pure forced convection with uniform wall temperature; ——— $\theta_w = 2$; - - - - $\theta_w = 0{\cdot}5$.

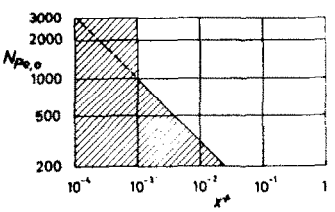

FIG. 14. Limits for the applicability of finite-difference solutions.

Less satisfactory is the result of a comparison with the measurements of Dalle Donne and Bowditch [6, 7] who found an exponent on the wall-to-bulk temperature ratio of 1·68.

Part of the discrepancies between the experimental values and those found by the present analysis may be due to the error introduced by the one-dimensional treatment of the flow in the reduction of the experimental data. Since, near the point of maximum wall-to-bulk temperature ratio, the velocity profile is considerably more flat than the parabolic profile where the heating starts, the acceleration of the flow will be underestimated and, consequently, too large a friction factor will be found.

CONCLUDING REMARKS

Due to the nonlinearity of the governing equations and the strong coupling between them the solutions presented in this paper do not have the generality of the classical solutions for flow with constant fluid properties. Still, some conclusions of general nature may be drawn from the present study.

It has been demonstrated that laminar flow of

gases in ducts, under conditions where large variations in the physical properties occur, can be described adequately by the boundary-layer equations. The basic restriction is of the same nature as for external boundary layers, namely that the Péclet number, based on axial distance, must be greater than a certain value, here found to be approximately 500. The significance of this result is that only due to the boundary layer approximations has it been possible to develop a fairly simple finite-difference scheme, giving reasonably short computation times.

At the rather small flow rates corresponding to laminar flow of gases, a high heating rate causes a rapid rise in the bulk temperature, and the wall-to-bulk temperature ratio will, therefore, approach unity relatively soon. Since it is this ratio, rather than the temperature difference, which determines the magnitude of the radial variation in the physical properties, significant temperature-dependent effects cannot persist beyond a certain distance from the start of the heating. The present solutions show that this distance largely coincides with the usual thermal-entry length for flow with constant properties. It follows that the concept of developed laminar flow with strong radial temperature gradients—the word "developed" referring to a situation where entrance effects are no longer present so that velocity and temperature profiles depend on local conditions only—is of quite limited practical significance with gases.

ACKNOWLEDGEMENTS

This paper is based on a dissertation [18] submitted to Stanford University by P. M. Worsøe-Schmidt in partial fulfillment of the requirements for the degree of Doctor of Philosophy. The ideas developed in the doctoral dissertation of Professor M. E. Davenport [22] led the authors to attempt this analysis, and the critical comments of Professor W. M. Kays were very helpful. The work was supported by U.S. Atomic Energy Commission under Contract AT(04-3)-247. P. M. Worsøe-Schmidt received financial support from The Technical University of Denmark and from Otto Mønsteds Fond as well as a travel grant under NATO's Science Fellowship Programme.

REFERENCES

1. R. G. Deissler, Analytical investigation of fully developed laminar flow in tubes with heat transfer with fluid properties variable along the radius, *NACA* Tech. Note 2410 (July 1951).
2. B. C. Sze, The effect of temperature dependent fluid properties on heat transfer in circular tubes. Ph.D. dissertation, Dept. Mech. Engng, Stanford University (April 1957).
3. M. E. Davenport and G. Leppert, The effect of transverse temperature gradients on the heat transfer and friction for laminar flow of gases, ASME paper 64-*HT*-10 (1964).
4. L. B. Koppel and J. M. Smith, Laminar flow heat transfer for variable physical properties, *J. Heat Transfer* **C84**, 157–163 (1962).
5. W. M. Kays and W. B. Nicoll, Laminar flow heat transfer to a gas with large temperature differences, *J. Heat Transfer* **C85**, 329–338 (1963).
6. M. Dalle Donne and F. H. Bowditch, High temperature heat transfer—Local heat transfer and average friction coefficients for laminar, transitional and turbulent flow of air in a tube at high temperature, *Nucl. Engng, Lond.* **8**, 20–29 (1963).
7. M. Dalle Donne and F. H. Bowditch, Experimental local heat transfer and friction coefficients for sub-sonic laminar, transitional, and turbulent flow of air and helium in a tube at high temperatures, OECD High Temperature Reactor Project Dragon, D.P. Rept 184 (April 1963).
8. Y. L. Wang and P. A. Longwell, Laminar flow in the inlet section of parallel plates, *J. Amer. Inst. Chem. Engrs* **10**, 323–329 (1964).
9. H. Schlichting, Laminäre Kanaleinlaufströmung, *Z. Angew. Math. Mech.* **14**, 368–373 (1934); also H. Schlichting, *Boundary Layer Theory*, 4th ed., p. 168. McGraw-Hill, New York (1960).
10. M. Collins and W. R. Schowalter, Laminar flow in the inlet region of a straight channel, *Phys. Fluids* **5**, 1122–1124 (1962).
11. M. Collins and W. R. Schowalter, Behavior of non-Newtonian fluids in the inlet region of a channel, *J. Amer. Inst. Chem. Engrs* **9**, 98–102 (1963).
12. J. R. Bodoia and J. F. Osterle, Finite-difference analysis of plane Poiseuille and Couette flow developments, *Appl. Sci. Res.* **A10**, 265–276 (1961).
13. R. Singh, Heat transfer by laminar flow in a cylindrical tube, *Appl. Sci. Res.* **A7**, 325–340 (1958).
14. P. J. Schneider, Effect of axial fluid conduction on heat transfer in the entrance region of parallel plates and tubes, *Trans. ASME* **78**, 765–773 (1957).
15. B. S. Petukhov and F. F. Tsvetkov, Calculation of heat transfer during laminar flow of a fluid in pipes within the range of small Péclet numbers, *Inzh.-Fiz. Zh.* **4**, 10–17 (1961). United Rough Draft Transl. *FTD-TT*-61-321/1+2 (January 1962).
16. I. Flügge-Lotz and F. G. Blottner, The solution of the laminar boundary-layer flow including displacement thickness interaction using finite-difference methods. Div. Engng Mech., Stanford University, Tech. Rept No. 131 (January 1962).
17. M. R. Abbott, Axially steady motion of a viscous incompressible fluid: Some numerical experiments, Royal Aircraft Establishment (Farnborough), Tech. Note No. Math. 98 (February 1963).
18. P. M. Worsøe-Schmidt, Finite-difference solution

for laminar flow of gas in a tube at high heating rate, Ph.D. dissertation, Dept. Mech. Engng, Stanford University (February 1965).
19. M. M. WENDEL and S. WHITAKER, Remarks on the paper "Finite-difference analysis of plane Poiseuille and Couette flow developments", by J. R. Bodoia and J. F. Osterle, *Appl. Sci. Res.* **A11**, 313–317 (1962).
20. T. J. HANRATTY, E. M. ROSEN and R. L. KABEL, Effect of heat transfer on flow field at low Reynolds numbers in vertical tubes, *Industr. Engng Chem.* **50**, 815–820 (1958).
21. W. G. BROWN, Die Überlagerung von erzwungener und natürlicher Konvektion in einem lotrechten Rohr, *Forschungsh. Ver. Dtsch. Ing.* 480 (1960).
22. M. E. DAVENPORT, The effect of transverse temperature gradients on the heat transfer and friction for laminar flow of gases, Ph.D. dissertation, Dept. Mech. Engng, Stanford University (July 1962).

APPENDIX

The application of the boundary-layer approximations for the present problem rests on purely heuristic arguments. The final justification must, therefore, be obtained by estimating the order of magnitude of the neglected terms from the numerical solutions. The two crucial assumptions are (i) that the molecular contributions to axial momentum and thermal energy transfer are negligible, and (ii) that the radial velocities are so small that all forces in the radial direction may be neglected.

The significance of the molecular transfer of momentum and thermal energy may be estimated from the magnitude of the terms

$$\frac{\partial}{\partial x}\left(\mu \frac{\partial u}{\partial x}\right) \quad \text{and} \quad \frac{\partial}{\partial x}\left(\frac{k}{c_p}\frac{\partial H}{\partial x}\right),$$

respectively, relative to the axial convection terms

$$\rho u \frac{\partial u}{\partial x} \quad \text{and} \quad \rho u \frac{\partial H}{\partial x}.$$

The magnitude of the forces acting in the radial direction is estimated from the radial inertia term

$$\rho u \frac{\partial v}{\partial x} + \rho v \frac{\partial v}{\partial r}$$

in comparison with the (axial) pressure gradient, representing the average magnitude of the forces in the axial direction.

The results of such estimates at $x^+ = 10^{-3}$ for $q^+ = 2$ and for $q^+ = 20$ are summarized in Table A.

Table A. Estimates of order of magnitude of neglected terms

	$q^+ = 2$	$q^+ = 20$
$\left\lvert \frac{\frac{\partial}{\partial x}\left(\mu \frac{\partial u}{\partial x}\right)}{\rho u \frac{\partial u}{\partial x}} \right\rvert_{\max}$	$\sim \frac{0{\cdot}4 \times 10^3}{N_{Pe,0}{}^2}$	$\sim \frac{10^4}{N_{Pe,0}{}^2}$
$\left\lvert \frac{\frac{\partial}{\partial x}\left(\frac{k}{c_p}\frac{\partial H}{\partial x}\right)}{\rho u \frac{\partial H}{\partial x}} \right\rvert_{\max}$	$\sim \frac{3 \times 10^3}{N_{Pe,0}{}^2}$	$\sim \frac{1{\cdot}5 \times 10^4}{N_{Pe,0}{}^2}$
$\frac{\left\lvert \rho u \frac{\partial v}{\partial x} + \rho v \frac{\partial v}{\partial r} \right\rvert_{\max}}{\left\lvert \frac{dP}{dx} \right\rvert}$	$\sim \frac{20}{N_{Pe,0}}$	$\sim \frac{50}{N_{Pe,0}}$

From the analogy to external boundary layers one would expect the applicability of the boundary-layer equations to be restricted by a minimum value of the Reynolds, or Péclet, number, based on the axial distance from the point where the heating starts. The connection between the two Péclet numbers, based on x and D, respectively, may be expressed as

$$x^+ = 2\, N_{Pe,x}/N_{Pe,0}^2$$

If we choose $(N_{Pe,x})_{\min} = 500$, the corresponding value of $N_{Pe,0}$ at $x^+ = 10^{-3}$ becomes 1000. It then follows from Table A that for $q^+ = 20$ the molecular contribution to axial momentum and thermal energy transfer are of the order of one to two per cent whereas for $q^+ = 2$ they are but a fraction hereof. The maximum value of the radial inertia term is for $q^+ = 20$ approximately five per cent of the typical force in the axial direction, decreasing to about two per cent for $q^+ = 2$.

In order to check the validity of using a fixed value of $N_{Pe,x}$ as criterion for the applicability of the approximations, the radial inertia term was also evaluated at $x^+ = 0{\cdot}008$ for $q^+ = 20$. This gave

$$\frac{\left\lvert \rho u \frac{\partial v}{\partial x} + \rho v \frac{\partial v}{\partial r} \right\rvert_{\max}}{\left\lvert \frac{dP}{dx} \right\rvert} \sim \frac{15}{N_{Pe,0}}$$

Corresponding to $N_{Pe,x} = 500$ we here find $N_{Pe,0} = 350$ and, hence, a relative magnitude of the radial forces of four to five per cent, nearly the same value as was found for $x^+ = 10^{-3}$.

Just as for incompressible flow in a plane duct, neglecting the radial momentum equation clearly is the most questionable of the approximations. However, the magnitude of the radial forces relative to the forces in the axial direction is still so small that we are justified in concluding that the boundary-layer approximations are indeed valid for the present problem as long as the Péclet number, based on axial distance, is greater than some 500.

Zusammenfassung—Für die Lösung des Problems der laminaren Gasströmung in beheizten (oder gekühlten) Kreisrohren mit einer unbeheizten Einlaufstrecke bei grossen Änderungen der Stoffwerte des Gases wurde ein implizites, endliches Differenzenverfahren entwickelt. Die Lösung basiert auf den Grenzschichtgleichungen, deren Gültigkeit für das vorliegende Problem mit den numerischen Lösungen nachgeprüft wurde.

Zahlenbeispiele wurden ausgearbeitet für Luft bei (i) reiner Zwangskonvektion mit verschiedenen Werten für konstante Beheizung; bei (ii) reiner Zwangskonvektion mit konstanter Wandtemperatur mit sowohl Aufheizen wie auch Abkühlen des Gases; und bei (iii) überlagerter Zwangs- und natürlicher Konvektion mit konstanter Wärmestromdichte. Für reine Zwangskonvektion werden Näherungsausdrücke für die lokale Nusseltzahl und den Reibungsbeiwert angegeben.

Аннотация—Разработана неявная схема конечных разностей для решения задачи ламинарного течения газов в нагретых (или охлажденных) кольцевых трубах с ненагреваемым входным участком в условиях больших изменений параметров газа. Решение основано на уравнениях пограничного слоя, справедливость которых для данной задачи проверена на численных решениях.

Разработаны численные примеры для воздуха, включая случаи: (i) вынужденной конвекции при различных скоростях равномерного нагрева; (ii) вынужденной конвекции при равномерной температуре стенки в случае нагревания и охлаждения газа; и (iii) совместной вынужденной и естественной конвекции при равномерном потоке тепла. Приведены приближенные выражения для локального критерия Нуссельта и коэффициента трения в случае вынужденной конвекции.